 CMES, vol.4, no.6, pp.679-689, 2003

Three-Dimensional Simulation of Turbulent Cavitating Flows in a Hollow-Jet Valve

Jiongyang Wu[1], Inanc Senocak[1], Guoyu Wang[2], Yulin Wu [3] and Wei Shyy[1]

Abstract: Cavitation appears in a wide variety of fluid machinery, and can often cause negative impacts on performance and structural integrity. A main computational difficulty for cavitation is the large density ratio between liquid and vapor phases, around 1000 for water under normal temperature and pressure conditions. Moreover, cavitating flows are usually turbulent and the interfacial dynamics is complex. The fast time scales associated with turbulent cavitation also poses substantial challenges computationally and experimentally. In the present study, pressure-based algorithms are adopted to simulate three-dimensional turbulent cavitating flows in a hollow-jet valve. The Favre-averaged Navier-Stokes equations are employed along with a transport equation-based cavitation model and the $k-\varepsilon$ two-equation turbulence model. Both steady state and time dependant computations are conducted. The time dependency of the flow field reflects the auto-oscillations of the cavity, formed at the needle tip of the hollow-jet valve. The pressure field throughout the flow domain, as well as the density field inside the cavity oscillates quasi-periodically in response to cavity oscillations. For the case investigated, the difference in the detailed cavitation dynamics between time dependent and steady state cases does not exhibit substantial influence on the overall flow pattern.

1 Introduction

Cavitation appears in a wide variety of fluid machinery like pumps, inducers, turbine blades, propellers and immersed hydrofoils. Pressure fluctuations, noise, power loss, vibrations and erosion are some of the pronounced effects of the cavitation phenomenon. It thus becomes imperative to gain insight into this phenomenon and as a result has been a topic of interest for many researchers. Athavale et al. (2000) adopted a vapor transport equation for vapor phase coupled with the turbulent N-S equations and reduced Rayleigh-Plesset equations to study of cavitation in pumps and inducers. To simulate the cavitating flows in rocket turbopump elements, Athavale and Singhal (2001) presented a homogeneous two-phase approach with a transport equation for vapor, again, using the reduced Rayleigh-Plesset equations for bubble dynamics and phase change rates. Medvitz et al. (2002) used multiphase computations to analyze the performance of centrifugal pumps under cavitating conditions. Duttweiler & Brennen (2002) experimentally investigated a previously unrecognized instability on a cavitating propeller in a water tunnel. The cavitation on the blades and in the tip vortices was explored through visual observation. Numerous other publications in the subject can be found in the references of the above-mentioned works and a recent review by Wang et al. (2001).

A main computational difficulty for cavitation is the large density ratio between the liquid phase and the vapor phase that can go up to 1000. Moreover, cavitating flows are usually turbulent and the interfacial dynamics involves complex interactions between vapor and liquid phases. The fast time scales associated with turbulent cavitation also poses substantial challenges to experimental observations. Multi-scale modeling and computational treatments typically utilize techniques such as averaging, matching, patching, or asymptotes. For references covering different fluid dynamics type of multi-scale problems, we refer to Shyy et al. (1997a, b), Martin et al. (1998), Shyy (2002), Garikipati (2002), and Wang et al. (2002).

In this present study, we focus on the cavitation phenomenon in flow-control valves. There are serious implications on the safe and sound operation for such issues. A limited number of experimental studies have been published on this topic, such as those by Oba et al. (1985)

[1] Department of Mechanical and Aerospace Engineering
University of Florida, Gainesville, FL, U.S.A.
[2] School of Vehicle and Transportation Engineering
Beijing Institute of Technology, Beijing, P.R.C.
[3] Department of Thermal Engineering
Tsinghua University, Beijing, P.R.C.

and Tani et al. (1991a, 1991b). In addition, Wang (1999) used high-speed cameras and Laser Light Sheet (LLS) to observe the cavitation behavior in a hollow-jet valve under various cavitation conditions and for different valve openings. However, to the best of our knowledge, to date, no comprehensive numerical study has been done in this respect. Furthermore, complex geometries and inaccessible regions of occurrence restrain experimental investigations in cavitation. In addition, we investigate the capability of transport equation-based cavitation models to predict incipient level cavitation.

In order to treat turbulent cavitating flows, we adopt a transport equation model for the volume or mass fraction, which allows coexistence of the liquid and vapor phases. Several recent studies have presented alternative modeling concepts and computational approaches based on this general idea. Singhal et al. (1997) employed a mass fraction equation with pressure dependent source terms. Kunz et al. (2000) utilized the artificial compressibility method with special focus on the preconditioning formulation. Ahuja et al. (2001) developed an algorithm to account for the compressibility effects in context of the artificial compressibility methods with use of adaptive unstructured grids. Senocak and Shyy (2002a) introduced a pressure-based algorithm to correct the density fields, which in turn was coupled with the $k-\varepsilon$ turbulence equations. Senocak and Shyy (2002b) developed an interfacial-dynamics-based model and appraised different cavitation models for N-S computation. They found that these alternative models gave qualitatively comparable and satisfactory predictions for the pressure distributions but quantitatively produced differences, such as phase fractions and pressure distributions, in the closure region of the cavity.

In SIMPLE-type of the pressure-based methods (Patankar 1980, Shyy 1994), the equations are solved successively by employing iterations. In cavitating flow computations, the typical relaxation factors used in the iterative solution process are smaller than the ones used in single-phase flows, and hence smaller time steps are needed to study the cavitation dynamics. Issa (1985) developed a method call the Pressure-Implicit with Splitting of Operator (PISO) for the solution of unsteady flows. The splitting of pressure and velocity makes the solution procedure sequential in time domain and enables the exact solution of the discretized equations to have a formal order of accuracy at each time step, and eliminates the need for severe under-relaxation in SIMPLE type algorithm. Bressloff (2001) extended the PISO for high-speed flows by adopting the pressure-density coupling procedure in all-speed SIMPLE type of methods. Oliveira and Issa (2001) followed the previous PISO work to combine the temperature equation to simulate buoyancy-driven flows. Thakur and Wright (2002) have developed approaches using curvilinear coordinates with suitability to all speeds. Senocak (2002) have further extended this PISO algorithm to enhance the coupling of cavitation and turbulence models and to handle the large density ratio associated with cavitation.

In this current study, we apply pressure-based algorithms, with the turbulence closure achieved by the $k-\varepsilon$ turbulence equations, combined with the Kunz et al.'s (2000) cavitation model, to simulate the turbulent cavitating flows in a hollow-jet valve. The single-phase steady state computations are handled using the extended SIMPLE type pressure-correction method (Shyy 1994). For cavitating flow simulations the pressure-based method, described in Senocak and Shyy (2002a), is used for steady state computations, and the pressure-based operator splitting method, described in Senocak (2002), is used for time-dependant computations. The numerical solutions and discussions are qualitatively assessed with the experimental observations from Wang (1999).

2 Theoretical formulation

2.1 Governing equations

The set of governing equations consists of the conservative form of the Favre-averaged Navier-Stokes equations, the $k-\varepsilon$ two-equation turbulence closure, and a volume fraction transport equation-based cavitation model. The mass continuity, momentum and cavitation model equations are given below:

$$\frac{\partial \rho_m}{\partial t} + \frac{\partial (\rho_m u_j)}{\partial x_j} = 0 \tag{1}$$

$$\frac{\partial (\rho_m u_i)}{\partial t} + \frac{\partial (\rho_m u_i u_j)}{\partial x_j} = -\frac{\partial p}{\partial x_i} + \frac{\partial}{\partial x_j}[(\mu+\mu_t)(\frac{\partial u_i}{\partial x_j} + \frac{\partial u_j}{\partial x_i} - \frac{2}{3}\frac{\partial u_k}{\partial x_k}\delta_{ij})] \tag{2}$$

$$\frac{\partial \alpha_l}{\partial t} + \frac{\partial(\alpha_l u_j)}{\partial x_j} = (\dot{m}^+ + \dot{m}^-) \tag{3}$$

The mixture density and turbulent viscosity are:

$$\rho_m = \rho_l \alpha_l + \rho_v (1-\alpha_l); \mu_t = \frac{\rho_m C_\mu k^2}{\varepsilon} \tag{4}$$

where α_l is the liquid volume fraction.

2.2 Cavitation modeling

Physically, the cavitation process is governed by the thermodynamics and the kinetics of the phase change process. The liquid-vapor conversion associated with the cavitation process is modeled through $\dot{m}^+$ and $\dot{m}^-$ terms in Eq.(3), which represents, respectively, condensation and evaporation. The particular form of these phase transformation rates are adopted from Kunz et al. (2000). Surface tension and buoyancy effects are neglected here considering the typical situation that the Weber and Froude numbers are large. The source terms adopted here are:

$$\dot{m}^- = \frac{C_{dest}\rho_v \alpha_l \mathrm{Min}(0, p-p_v)}{\rho_l (\rho_l U_\infty^2/2) t_\infty}$$

$$\dot{m}^+ = \frac{C_{prod}\rho_v \alpha_l^2 (1-\alpha_l)}{\rho_l t_\infty} \tag{5}$$

where $C_{dest} = 9.0 \times 10^5$ and $C_{prod} = 3.0 \times 10^4$ are empirical constant values, $U_\infty$is a characteristic velocity scale, here it is chosen as the inlet value. The time scale in the equation is defined as the ratio of the characteristic length scale to the reference velocity scale (D/U). The nominal density ratio (ρ_v/ρ_l) is the ratio between thermodynamic values of density of vapor and liquid phases at the corresponding flow condition.

2.3 Turbulence modeling

For the system closure, the original $k-\varepsilon$ turbulence model with wall functions is presented as follows:

$$\frac{\partial(\rho_m k)}{\partial t} + \frac{\partial(\rho_m u_j k)}{\partial x_j} = \mathrm{P}_t - \rho_m \varepsilon + \frac{\partial}{\partial x_j}[(\mu + \frac{\mu_t}{\sigma_k})\frac{\partial k}{\partial x_j}] \tag{6}$$

$$\frac{\partial(\rho_m \varepsilon)}{\partial t} + \frac{\partial(\rho_m u_j \varepsilon)}{\partial x_j} = C_{\varepsilon 1}\frac{\varepsilon}{k}\mathrm{P}_t - C_{\varepsilon 2}\rho_m \frac{\varepsilon^2}{k} + \frac{\partial}{\partial x_j}[(\mu + \frac{\mu_t}{\sigma_\varepsilon})\frac{\partial \varepsilon}{\partial x_j}] \tag{7}$$

The turbulent production, Reynolds stress tensor terms, and the Boussinesq eddy viscosity concept are defined:

$$\mathrm{P}_t = \tau_{ij}\frac{\partial u_i}{\partial x_j}$$

$$\tau_{ij} = \overline{-\rho u_i' u_j'}$$

$$\overline{u_i' u_j'} = \frac{2k\delta_{ij}}{3} - \nu_t(\frac{\partial u_i}{\partial x_j} + \frac{\partial u_j}{\partial x_i}) \tag{8}$$

In the above equations, coefficients $C_{\varepsilon 1} = 1.44$, $C_{\varepsilon 2} = 1.92$, $\sigma_\varepsilon = 1.3$, $\sigma_k = 1.0$ are empirical constants.

2.4 Dimensionless parameters

The non-dimensional parameters of interest in this report, including Reynolds number, cavitation number and the pressure coefficient, are defined in the following:

$$Re = \frac{\rho_l U_\infty D}{\mu_l} \tag{9}$$

$$\sigma = \frac{P_2 - P_v}{\frac{1}{2}\rho_l V^2} \tag{10}$$

$$C_p = \frac{P - P_2}{\frac{1}{2}\rho_l U_\infty^2} \tag{11}$$

Here, ρ_l, μ_l are liquid density and viscosity, D is the diameter of the valve needle, $V$is the mean flow velocity at the valve section through the needle seal (tip), $P_2$is the outlet pressure,P_v is the saturated vapor pressure. The definition of cavitation number σ is taken as that in Wang (1999).

3 Numerical method

The present Navier-Stokes solver employs pressure-based algorithms and the finite volume approach (Shyy 1994, Shyy et al. 1997a). The governing equations are

solved on multi-block structured curvilinear grids. To represent the cavitation dynamics, a transport equation model is adopted along with the particular source terms as suggested by Kunz et al (2000). The pressure-based method described in Senocak and Shyy (2002a) is utilized for steady-state computations of turbulent cavitating flows. One of the key features of this method is to reformulate the pressure correction equation to exhibit a convective-diffusive nature. Here we summarize some key computational issues by focusing on the flux terms in the continuity equation, which can be decomposed as follows:

$$\begin{aligned}\rho\vec{u} &= (\rho^* + \rho')(\vec{u}^* + \vec{u}') \\ &= \rho^*\vec{u}^* + \rho^*\vec{u}' + \rho'\vec{u}^* + \rho'\vec{u}' \end{aligned} \tag{12}$$

where the starred variables represent the predicted values and primed variables represent the correction terms. The substitution of the flux terms in the discretized continuity equation leads to the following convective-diffusive type pressure correction equation.

$$\begin{aligned}&-\nabla_d \cdot (\rho^* D \nabla_d P') + \nabla_d \cdot (C_\rho \vec{u}^* P') \\ &\quad = -\nabla_d \cdot (\rho^* \vec{u}^*) + \nabla_d \cdot (C_\rho P'_p D \nabla_d P')\end{aligned} \tag{13}$$

$$\rho'_p = C_\rho P'_p \tag{14}$$

The relative importance of the first and second terms in Eq.(10) depends on the local Mach number (Shyy 1994). For low Mach number flows, only first term prevails; for high Mach number flows, the second term dominates. The fourth term is a nonlinear second-order term and can be either neglected or included in the source term for stability in early iterations. In the present algorithm, the following relation between density and pressure correction is taken as suggested in Senocak and Shyy (2002a)

$$\rho'_p = C(1-\alpha_l)_p P'_p \tag{15}$$

where C is an arbitrary constant which does not affect the final converged solution due to the pressure correction nature.

For unsteady flow computations, PISO algorithm is used. In this algorithm the system of discretized equations are solved through predictor and corrector steps without the need for iteration. In the following we summarize the basic steps of the algorithm. A detailed description of the algorithm for turbulent cavitating flow computations is documented in Senocak (2002).

In the predictor step the discretized momentum equations are solved implicitly using the old time pressure to obtain an intermediate velocity field. A backward Euler scheme is used for the discretization of the time derivative term

$$\vec{u}^*_p = H[\vec{u}^*]_p - D_p(\nabla_d P^{n-1})_p + \frac{(\rho\vec{u})^{n-1}}{\delta t} \tag{16}$$

The intermediate velocity field does not satisfy continuity and needs to be corrected using the continuity equation as a constraint. In the first corrector step, a new velocity field, $\vec{u}^{**}$ and pressure field $P^*$are expected. The following convective-diffusive type pressure correction equation is solved in the first corrector step.

$$\begin{aligned}&\frac{C_\rho P'_p}{\delta t} V_p - \Delta[\rho^{n-1} D(\nabla_d P') \cdot \vec{n} S_{cf}]_p + \Delta[C_\rho P' U^*]_p \\ &= -\Delta[\rho^{n-1} U^*]_p\end{aligned} \tag{17}$$

In the second corrector step the following convective – diffusive type pressure correction equation is solved to satisfy the mass conservation.

$$\begin{aligned}&\frac{C_\rho P''_p}{\delta t} V_p - \Delta[\rho^* D(\nabla_d P'') \cdot \vec{n} S_{cf}]_p + \Delta[C_\rho P'' U^{**}]_p \\ &= -\Delta[\rho^* U^{**}]_p - \Delta[\rho^* \mathbf{H}[\vec{u}^{**} - \vec{u}^*] \cdot \vec{n} S_{cf}]_p\end{aligned} \tag{18}$$

Then, through solving the above predictor and correction steps coupled with the cavitation and turbulence model equations the solution procedure for turbulent cavitating flow computations is accomplished.

For unsteady cavitating flow computations, the pressure-density coupling scheme becomes important. Senocak (2002) have discussed the issue by studying unsteady cavitation in convergent-divergent nozzles. We adopt the following scheme as suggested by Senocak (2002).

$$C_\rho = (\frac{\partial \rho}{\partial P})_s = \frac{1}{c^2} \approx (\frac{\Delta\rho}{\Delta P})_\xi = \frac{|\rho_{i+1} - \rho_{i-1}|}{|P_{i+1} - P_{i-1}|} \tag{19}$$

For further details of the numerical method adopted in this study the reader is referred to Senocak and Shyy (2002a) and Senocak (2002).

4 Results and discussions

As documented in Wang (1999), Figure 1 shows the geometry and the main configurations of the valve. A key

component is the needle, used to control the flow rate. A cylindrical seal supports the needle. There are six struts supporting the cylinder, which are called splitters. The gear is used to control the needle position moving through the X-axis.

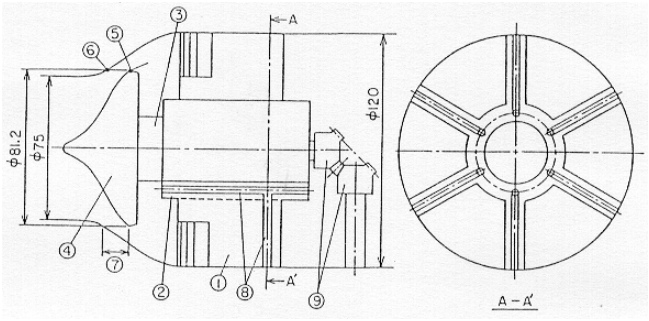

Figure 1 : Geometry of the valve. (1) Splitter; (2) Cylinder; (3) Plunger; (4) Needle; (5) Needle seal overlay; (6) Seal seat inlay; (7) Stroke; (8) Ventilation duct; (9) Gear

Figure 2 illustrates the computational domain in selected planes according to the geometry. A multi-block structured curvilinear grid is adopted to facilitate the computation. Figure 2-a shows the configuration on the X-Y plane, and Figure 2-b from the Y-Z plan. Figure 2-c shows the planes location, and Figure 2-d shows the boundary conditions in the computations. Here, the splitter thickness is neglected and its shape is considered to be rectangular. The Reynolds number is $5\times10^5$and the cavitation number is 0.9, with the density ratio between the liquid phase and vapor phase ρ_l/ρ_v being 1000. Both time dependent and steady state computations are conducted with a valve opening of 33%, using non-dimensional equations. For the time dependent case, the steady single-phase turbulent flow, without considering cavitation, is computed and the solution is adopted as the initial condition for the unsteady cavitating turbulent flow. The results and discussion are presented in the following.

Figure 3 shows the density distributions for the steady case. The cavities on the splitter plane and the middle plane are slightly different in size. Figure 4 shows how the cavity shape and location vary with time growing. In 5, four instantaneous solutions are selected.

For time dependent computations, the cavity fluctuates quasi-periodically. At the non-dimensional time $t^* = 0.4$, the cavity is the biggest with smallest density, see Figure

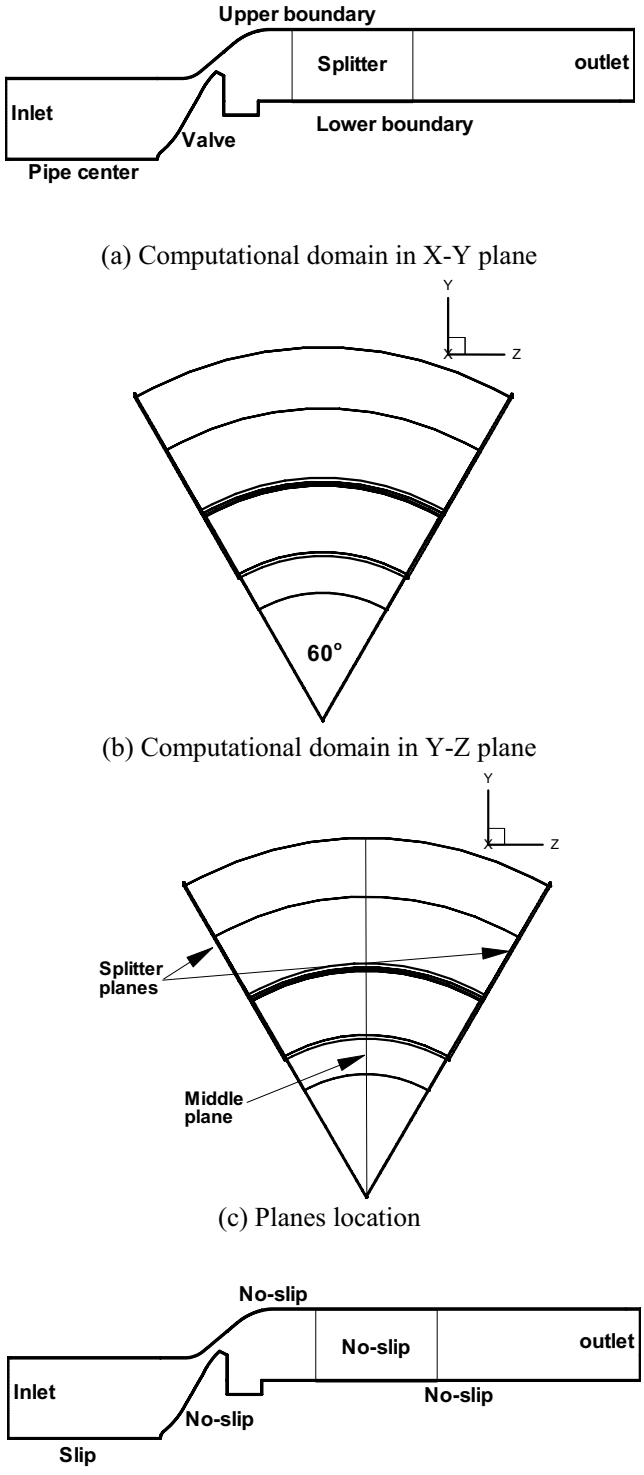

Figure 2 : Computational domains and boundary conditions

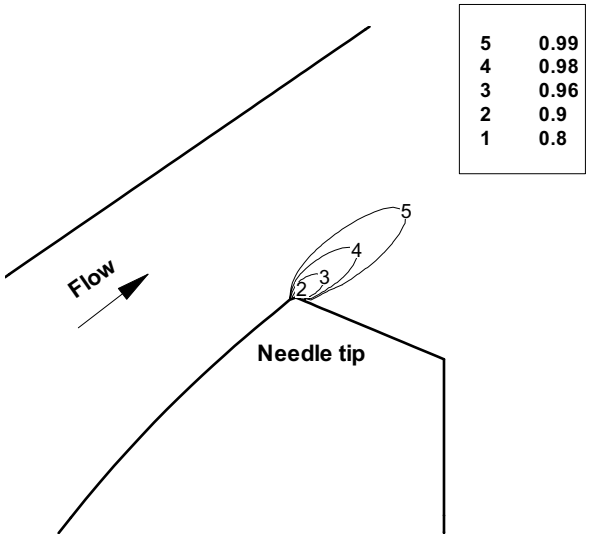

(a) At splitter plane

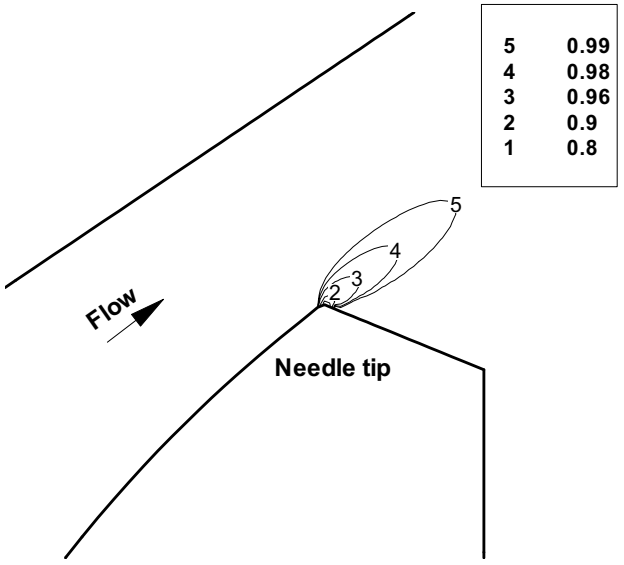

(b) At middle plane

Figure 3 : Density contour lines of the steady state solution. The mixture of vapor and liquid inside the outer line forms the cavity.

4-a. With time growing, the size reduces to the smallest, as Figure 4-b & Figure 4-c at time $t^* = 0.6$ and $t^* = 0.8$, respectively. Then after one cycle it reaches the maximum again, as shown in Figure 4-d at $t^* = 1.2$. Both steady and unsteady results exhibit the cavity at the needle tip, as depicted in Figure 3 & Figure 4. The steady case corresponds to a single instantaneous result in the time dependent solution (Figure 3-b and Figure 4-c). The time dependent results are qualitatively consistent with experiment in size and shape, as illustrated in Figure 4-a (or Figure 4-d) and Figure 4-e. Unfortunately, there is insufficient experimental information to ascertain the time dependent characteristics in detail.

In the experiments it has been observed that the cavities incept, grow, then detach from the needle tip and transport to the downstream periodically, as clearly shown in Figure 4-e the cavitation aspects around the needle. However, as already discussed in Senocak (2002) for unsteady cavitation in convergent-divergent nozzles, with the current combination of turbulence and cavitation models, the detachment of the cavity is not captured, possibly due to the representation of the turbulence via a scalar eddy viscosity.

To further demonstrate the cavity-induced quasi-periodic characteristics of the flow field, 5 highlights the time evolutions at selected locations. 5-a shows the locations of the points selected. The pressure is at the middle points, and the density is near the bottom boundary, just one point away from it. From 5-b, at the places far away from the cavity, A, B and D, the density is constant since only the liquid phase exists there, and is quasi-periodic inside the cavity at Point C. On the other hand, as shown in 5-c, pressure oscillates in the whole domain except on the outlet plane, where the flow condition is fixed.

Figure 6 presents the flow structure on the middle plane. For the steady case, the flow fields of both single phase (without invoking the cavitation model in the course of computation) and cavitating flows are almost identical, as shown in Figure 6-a. It indicates that in the present case, the incipient level cavitation dynamics does not exhibit substantial influence on the overall flow pattern. For the time dependent case, at difference time instants, Figure 6-b $t^* = 0.4$ and $t^* = 0.8$, the flow field around the needle remains largely the same. The comparison between the steady and unsteady case points out that there does not exist very much difference in the flow pattern. As expected, there are two recirculating zones: one behind the

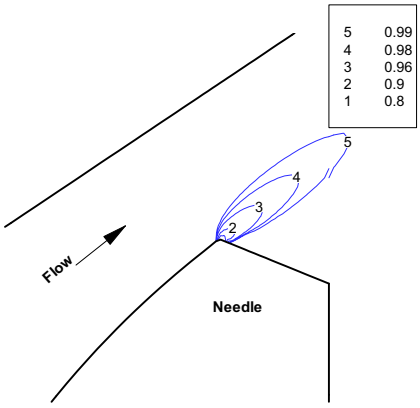

(a) Time $t^* = 0.4$

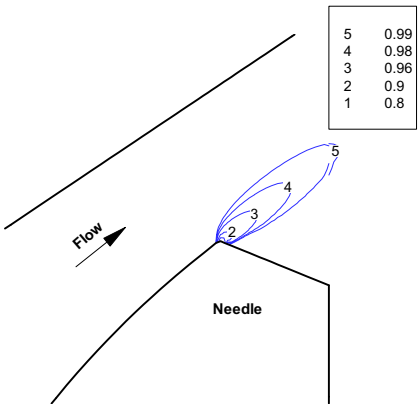

(b) Time $t^* = 0.6$

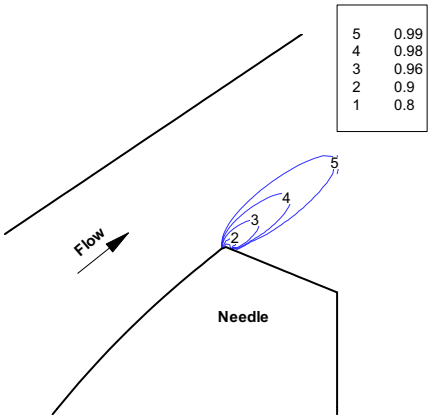

(c) Time $t^* = 0.8$

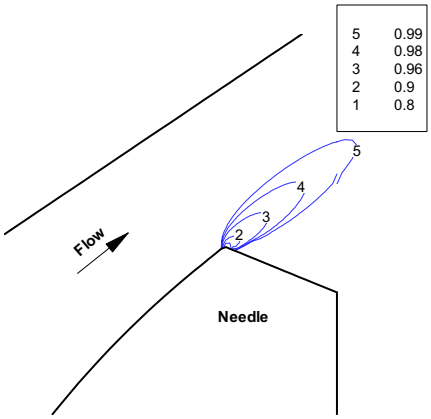

(d) Time $t^* = 1.2$

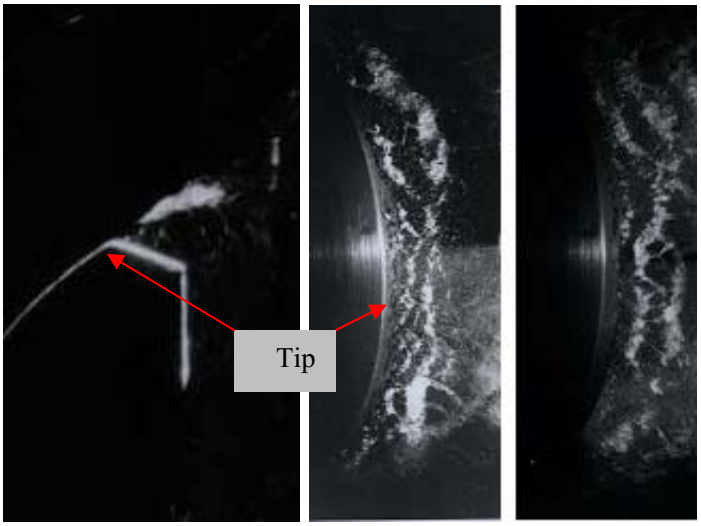

(e) Experimental observations: cavity at needle tip (left) & cavitation aspects around the needle (right)

Figure 4 : Middle section density contours at different time instants. The mixture of vapor and liquid inside the outer line forms the cavity.

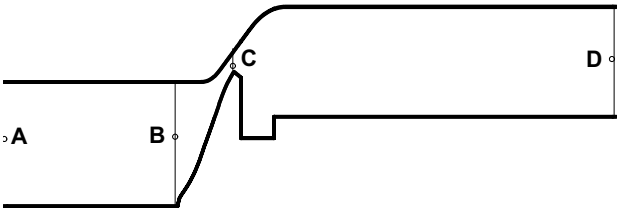

(a) Samples locations, A—inlet; B—needle leading; C—needle tip; D--outlet

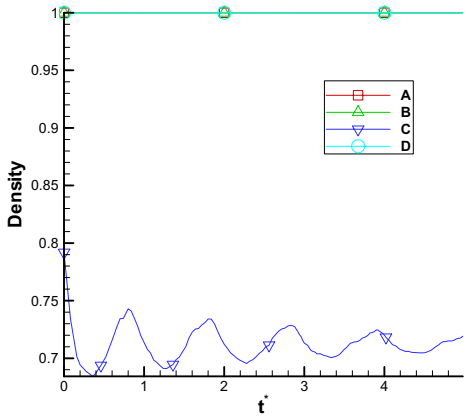

(b) Density

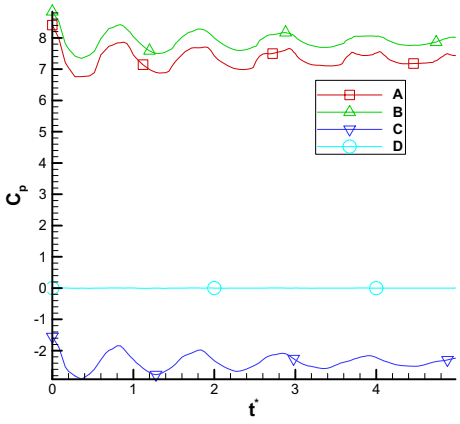

(c) Pressure

Figure 5 : Time evolution at different locations

needle and the other one downstream around the splitter region, which locates about at x=3.4∼4.2. Comparing with the experimental observation (Figure 6-c is the cavitating flow structures behind the needle, and Figure 6-d is the cavitating flow structures in the splitter region), the present results are in general agreement.

5 Conclusions

In the current study, unified pressure-based algorithms have been used to simulate the turbulent cavitating flow in a hollow-jet valve. Both steady state and time dependent solutions exhibit qualitatively comparable flow patterns and cavity sizes. The time dependency of the flow field is demonstrated by the auto-oscillations of the cavity, formed at the needle tip of the hollow-jet valve. The upstream and downstream pressures oscillate quasi-periodically in response to cavity oscillations. Two recirculating zones are observed; one behind the needle and the other at the splitter region. These numerical results agree quantitatively with the experimental results. Observing the steady state and time dependent solutions, it appears that for the present geometry and flow regime, the incipient level cavitation dynamics does not exhibit substantial influence on the overall flow pattern.

The work presented here will be further extended to account for fluid dynamics and rotordynamics interactions. Such models will require coupling between fluid dynamics and structural dynamics (see, e.g., Kamakoti et al. 2002), including possibly boundary movement (Shyy et al. 1996). Once this level of model is developed, we will attain much improved capability to conduct design optimization of fluid machinery, which will further advance the state-of-the arts (Levin and Shyy 2001, Papila et al. 2002, Shyy et al. 2001) in this general area.

Acknowledgement: The present study has been supported in part by NASA and ONR.

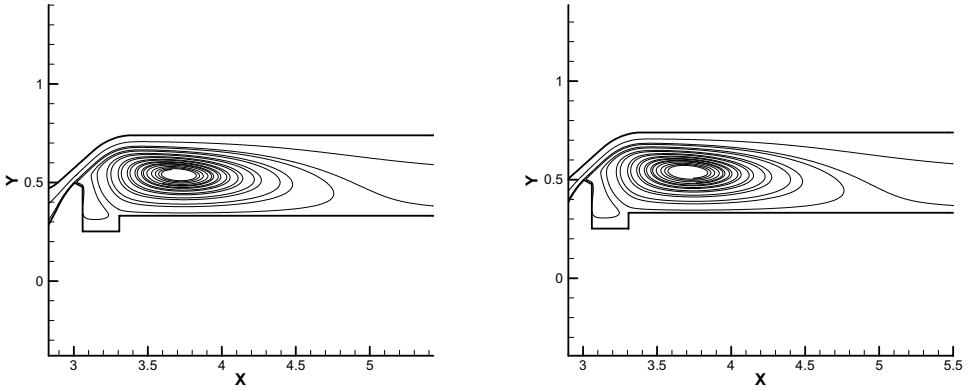

(a) The steady flow streamlines at middle section, single phase flow (left) and cavitating flow (right)

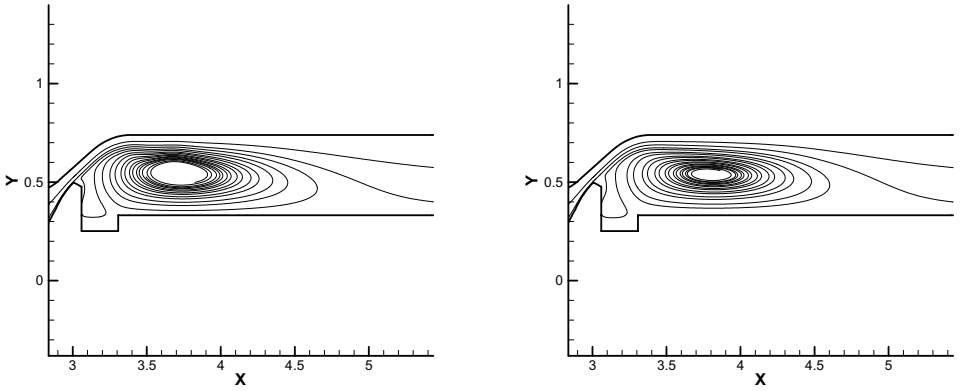

(b) The unsteady cavitating flow streamlines on the middle section, at time $t^* = 0.4$ (left) & $t^* = 0.8$ (right)

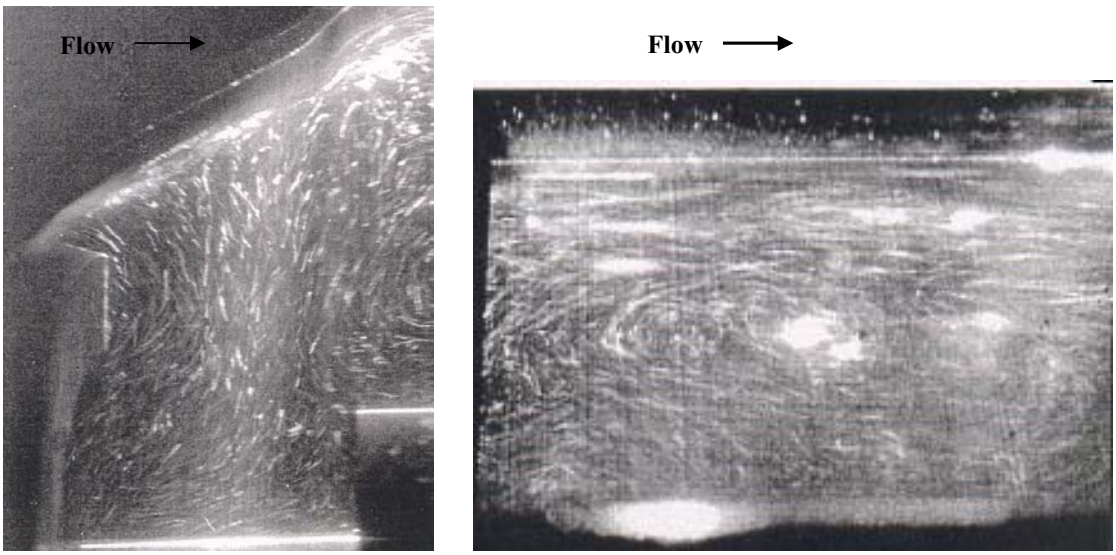

(c) Flow pattern behind valve

(d) Flow pattern at splitter region, about x=3.4~4.2

Figure 6 : Projected 2-D streamlines at middle plane & experiment results

References

Ahuja, V.; Hosangadi, A.; Arunajatesan, S. (2001): Simulations of Cavitating Flows Using Hybrid Unstructured Meshes, *J. of Fluids Engineering*, vol. 123, pp. 331-340.

Athavale, M. M.; Li, H. Y.; Jiang, Y.; Singhal, A. K. (2000): Application of the Full Cavitation Model to Pumps and Inducers, *paper of the 8th International Symposium on Transport Phenomena and Dynamics of Rotating Machinery (ISEOMAC-8)*

Athavale, M. M.; Singhal, A. K (2001): Numerical Analysis of Cavitating Flows in Rocket Turbopump Elements, *AIAA-2001-3400*.

Bressloff, N. W. (2001): A Parallel Pressure Implicit Splitting of Operator Algorithm Applied to Flows at All Speed, *Int. J. Numer . Meth. Fl.*, vol. 36 (2), pp. 497-518.

Duttweiler, M. E.; Brennen, C. E. (2002): Surge Instability on a Cavitating Propeller, *J. Fluid Mech.*, vol. 458, pp. 133-152.

Garikipati, K. (2002): A Variational Multiscale Method to Embed Micromechanical Surface Laws in the Macromechanical Continuum Formulation, *CMES: Computer Modeling in Engineering & Sciences*, vol. 3, no. 2, pp. 175-184.

Issa, R. I. (1985): Solution of the Implicitly Discretised Fluid Flow Equations by Operator-Splitting, *J. Comput. Phys.*, vol. 62, pp. 40-65.

Kamakoti, R.; Lian, Y.; Regisford, S.; Kurdila, A.; Shyy, W. (2002): Computational Aeroelasticity Using a Pressure-Based Solver. Accepted by *CMES: Computer Modeling in Engineering & Sciences*.

Kunz, R. F.; Boger, D. A.; Stinebring, D. R.; Chyczewski, T. S.; Lindau, J. W.; Gibeling, H. J.; Venkateswaran, S.; Govindan, T. R. (2000): A Preconditioned Navier-Stokes Method for Two-Phase Flows with Application to Cavitation Prediction, *Computers & Fluids*, vol. 29, pp. 849-875.

Levin, O. and Shyy, W. (2001): Optimization of a Flexible Low Reynolds Number Airfoil, *CMES: Computer Modeling in Engineering & Sciences*, vol. 2, pp. 523-536.

Martin, A. R.; Saltiel, C.; Shyy, W. (1998): Frictional Losses and Convection Heat Transfer in Sparse, Periodic Cylinder Arrays in Cross Flow, *International Journal of Heat and Mass Transfer*, vol. 41, pp. 2383-2397.

Medvitz, R. B.; Kunz, R. F.; Boger, D. A.; Lindau, J. W.; Yocum, A. M. (2002): Performance Analysis of avitating Flow in Centrifugal Pumps Using Multiphase CFD, *J. Fluids Eng.*, vol.124, pp. 377-383.

Oba, R.; Ito, Y.; Miyakura, H. (1985): Cavitation Observation in a Jet-Flow Gate-Valve, *JSME Int. J.*, Series B, vol. 28, pp. 1036-1043.

Oliveira, P. J.; Issa, R. I. (2001): An Improved PISO Algorithm for the Computation of Buoyancy-Driven Flows, *Numerical Heat Transfer, Part B*, vol. 40, pp. 473-493.

Papila, N.; Shyy, W.; Griffin, L.; Dorney, D. J. (2002): Shape Optimization of Supersonic Turbines Using Global Approximation Methods, *Journal of Propulsion and Power*, vol. 18, pp. 509-518.

Patankar, S. V. (1980): *Numerical Heat Transfer and Fluid Flow*, Hemisphere, Washington, D.C.

Senocak, I. (2002): *Computational Methodology for the Simulation of Turbulent Cavitating Flows*, Ph.D. Dissertation, University of Florida, Gainesville, USA.

Senocak, I. and Shyy, W. (2002a): A Pressure-Based Method for Turbulent Cavitating Flow Computations, *J. of Comp. Physics*, vol.176, pp. 363-383.

Senocak, I. and Shyy, W. (2002b): Evaluation of Cavitation Models for Navier-Stokes Computations, FEDSM2002-31011, *Proc. of 2002 ASME Fluids Engineering Division Summer Meeting* Montreal, CA.

Shyy, W. (1994): *Computational Modeling for Fluid Flow and Interfacial Transport*, Elsevier, Amsterdam, The Netherlands (Revised print 1997).

Shyy, W.; Udaykumar, H. S.; Rao, M. M. and Smith, R. W. (1996): *Computational Fluid Dynamics with Moving Boundaries*, Taylor & Francis, Washington, DC, (revised print 1997, 1998 & 2001).

Shyy, W.; Thakur, S. S.; Ouyang, H.; Liu, J.; Blosch, E. (1997a): *Computational Techniques for Complex Transport Phenomena*, Cambridge University Press, New York.

Shyy, W.; Liu, J.; Ouyang, H. (1997b): Multi-Resolution Computations for Fluid Flow and Heat/Mass Transfer, in *Advances in Numerical Heat Transfer*, Minkowycz, W. J., and Sparrow, E. M. (editors), vol. 1, pp. 137-169, Taylor & Francis, Washington, DC.

Shyy, W.; Papila, N.; Vaidyanathan, R.; Tucker, P.K. (2001): Global Design Optimization for Aerody-

namics and Rocket Propulsion Components, *Progress in Aerospace Sciences*, vol. 37, pp. 59-118.

Shyy, W. (2002): Multi-Scale Computational Heat Transfer with Moving Solidification Boundaries, *International Journal for Heat and Fluid Flow*, vol. 23, pp. 278-287.

Singhal, A. K.; Vaidya, N.; Leonard, A. D. (1997): Multi-Dimensional Simulation of Cavitating Flows Using a PDF Model for Phase Change, ASME paper FEDSM97-3272, *Proc. of 1997 ASME fluids Engineering Division Summer Meeting*.

Tani, K.; Ito, Y.; Oba, R.; Yamada, M.; Onishi, Y. (1991a): High-Speed Stereo-Flow Observations around a Butterfly Valve, *Mem. Inst. Fluid Sci.*, Tohoku Univ., vol. 2, pp. 101-112.

Tani, K.; Ito, Y.; Oba, R.; Iwasaki, M. (1991b): Flow Visualization in the High Shear Flow on Cavitation Erosion around a Butterfly Valve, *Trans. JSME*, vol. 57, pp. 1525-1529.

Thakur, S. S.; Wright, J. F. (2002): An Operator-Splitting Algorithm for Unsteady Flows at All Speed in Complex Geometries, to be published.

Wang, G. (1999): *A Study on Safety Assessment of a Hollow-Jet Valve Accompanied with Cavitation*, PhD Dissertation, Tohoku University, Sendai, Japan.

Wang, G.; Senocak, I.; Shyy, W.; Ikohagi, T.; Cao, S. (2001): Dynamics of Attached Turbulent Cavitating Flows, *Progress in Aerospace Sciences*, vol. 37, pp. 551-581.

Wang, Y.; Wang, Q. J.; Lin, C. (2002): Mixed Lubrication of Coupled Journal-Thrust Bearing Systems, *CMES: Computer Modeling in Engineering & Sciences*, vol. 3, no. 4, pp. 517-530.